

Micromachined pressure sensors: review and recent developments

To cite this article: W P Eaton and J H Smith 1997 *Smart Mater. Struct.* **6** 530

View the [article online](#) for updates and enhancements.

Related content

- [MEMS-based pressure and shear stress sensors for turbulent flows](#)
Lennart Löfdahl and Mohamed Gad-el-Hak
- [Group III nitride and SiC based MEMS and NEMS](#)
V Cimalla, J Pezoldt and O Ambacher
- [A review: crystalline silicon membranes over sealed cavities for pressure sensors by using silicon migration technology](#)
Jiale Su, Xinwei Zhang, Guoping Zhou et al.

Recent citations

- [N. Kalayzhaçan et al](#)
- [Basilar membrane-inspired self-powered acoustic sensor enabled by highly sensitive multi tunable frequency band](#)
Jae Hyun Han et al
- [Microdevice Development and Artificial Organs](#)
Jeffrey D. Zahn

Micromachined pressure sensors: review and recent developments

W P Eaton† and J H Smith

Intelligent Micromachines Department, Sandia National Laboratories, Albuquerque, NM 87185-1080, USA

Received 25 April 1997, accepted for publication 28 May 1997

Abstract. Since the discovery of piezoresistivity in silicon in the mid 1950s, silicon-based pressure sensors have been widely produced. Micromachining technology has greatly benefited from the success of the integrated circuit industry, borrowing materials, processes, and toolsets. Because of this, microelectromechanical systems (MEMS) are now poised to capture large segments of existing sensor markets and to catalyse the development of new markets. Given the emerging importance of MEMS, it is instructive to review the history of micromachined pressure sensors, and to examine new developments in the field. Pressure sensors will be the focus of this paper, starting from metal diaphragm sensors with bonded silicon strain gauges, and moving to present developments of surface-micromachined, optical, resonant, and smart pressure sensors. Considerations for diaphragm design will be discussed in detail, as well as additional considerations for capacitive and piezoresistive devices. Results from surface-micromachined pressure sensors developed by the authors will be presented. Finally, advantages of micromachined sensors will be discussed.

1. Introduction

Microelectromechanical systems (MEMS) have received a great deal of attention in recent years. This is due not only to the excitement naturally associated with a nascent technology, but also because of the great promise of increased miniaturization and performance of MEMS devices over conventional devices. MEMS pressure sensors currently dominate the market for greater-than-atmospheric-pressure sensors. The 1995 market for micromachined pressure sensors was approximately \$US 1 billion, and is expected to grow to \$US 2.5 billion by 2005 [1].

While the focus of this paper is a review of micromachined pressure sensors, it is instructive to first examine macroscopic devices, since many micromachined sensors are miniaturized versions of their larger counterparts. Several macroscopic sensors are shown in figure 1. The common feature of all of these sensors was that they converted pressure to motion of a mechanical element. Many devices were based on diaphragms (a, b, d). Other devices sought to improve the amount of deflection of a simple diaphragm such as the capsule (c) and bellows (e). Strain gauges were commonly used on diaphragm based devices. Some diaphragm sensors, however, had elaborate systems of levers which were linked to electric switches or potentiometer windings. Some diaphragm sensors, instead of having strain gauges mounted directly on the diaphragm itself, had a piston which was driven into a mounted strain

gauge by the motion of the diaphragm. Finally Bourdon tubes and straight-walled tubes deflected or expanded in the presence of increased pressure (f, g).

Vacuum pressure sensors typically use different transduction mechanisms than their greater-than-atmosphere-pressure counterparts. A Pirani gauge measures the thermal conductivity of the ambient gas, which is directly proportional to pressure in the 1–2000 mTorr range [2]. A heated resistor is used for this measurement. Ionization gauges operate at pressures from 1 mTorr down to 2×10^{-8} Torr [2]. In these gauges, electrons are emitted from a cathode and accelerated towards an anode plate. Positive ions are created by electron–gas collisions. These ions are attracted to a third plate. The current on this plate is proportional to the absolute pressure of the gas.

2. Micromachined pressure sensors

As noted before, many micromachined pressure sensors are miniaturized versions of their macroscopic counterparts. A micromachined Pirani gauge has been reported for measuring vacuum [3]. Similarly, most sensors for greater-than-atmospheric pressure share the common characteristic of deformable diaphragms. In diaphragm-based sensors, pressure is determined by the deflection of the diaphragms due to applied pressure. Figure 2 illustrates a schematic cross section of a typical pressure sensor diaphragm. The reference pressure can be a sealed chamber or a pressure port so that absolute or gauge pressures are measured, respectively. The shape of the diaphragm as viewed from

† Present address: Reliability Physics Department, Sandia National Laboratories, Albuquerque, NM 87185-1081, USA.

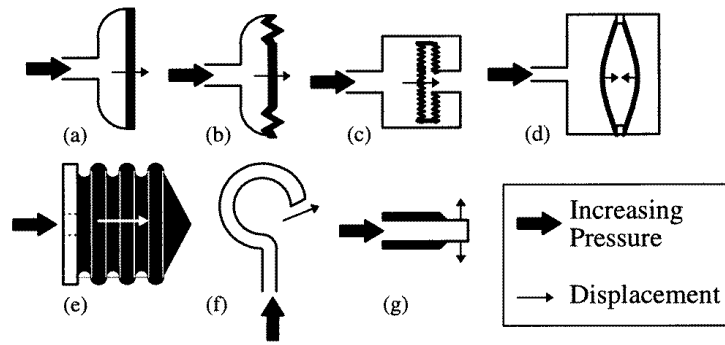


Figure 1. Macroscopic pressure sensors (adapted from [2]): (a) simple diaphragm; (b) corrugated diaphragm; (c) capsule; (d) capacitive sensor, (e) bellows; (f) Bourdon tube; (g) straight tube.

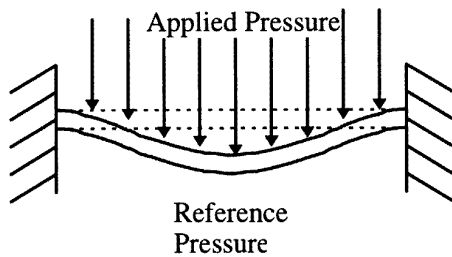


Figure 2. A schematic cross section of a typical pressure sensor diaphragm. Dotted lines represent the undeflected diaphragm.

the top is arbitrary, but generally takes the form of a square or circle. These shapes behave similarly for a given applied stress. For the case of a clamped circular plate with small deflections (i.e., less than half of the diaphragm thickness) the form of the deflection is [4]

$$w(r) = \frac{Pa^4}{64D} \left[1 - \left(\frac{r}{a} \right)^2 \right]^2 \quad (1)$$

where w , r , a , and P are the deflection, radial distance from the centre of the diaphragm, diaphragm radius, and applied pressure, respectively. D is the flexural rigidity, given by

$$D = \frac{Eh^3}{12(1-\nu^2)} \quad (2)$$

where E , h , and ν are the Young's modulus, thickness, and Poisson's ratio, respectively, of the diaphragm. From the above equations it is readily apparent that the amount of deflection is directly proportional to the applied pressure. For the case of a diaphragm with large built-in stress or large deflections, however, this direct proportionality no longer holds true. In general, it is often desirable to use a deflection measurement scheme that is linear with pressure, since such systems are simple to calibrate and measure.

In this paper several types of micromachined pressure sensor are reviewed, as classified by transduction mechanisms. Most of the emphasis will be placed upon capacitive and piezoresistive sensors, since they are the most common, with lesser emphasis on optical and resonant devices. Also, microphones and hydrophones, which are related to pressure sensors, will be briefly reviewed. Details

of MEMS fabrication processes are beyond the scope of this paper, and have been discussed by Mastrangelo and Tang [5]. However, a brief discussion of MEMS materials follows.

2.1. Materials

The quality and reproducibility of constituent materials play a critical role in the commercial viability of pressure sensors. The focus of this paper will be bulk and surface micromachining, where the desired mechanical structures are made from the substrate itself, or thin films deposited on the substrate, respectively.

2.1.1. Bulk micromachining. In bulk micromachining one of the dominant materials is single-crystal silicon. The mechanical properties of single-crystal silicon are excellent, as reported in a landmark article by Petersen in 1982 [6]. It has high strength, high stiffness, high mechanical repeatability, high Q , and no mechanical hysteresis. Furthermore, single-crystal silicon is available in large quantities with high purity and low defect densities. Piezoresistive gauge factors in silicon are higher than in metal, but temperature coefficients of resistance (TCRs) are high. Because of high TCRs, silicon microsensors often require temperature compensation techniques [1].

2.1.2. Surface micromachining. Surface-micromachining materials do not have the same high quality as single-crystal silicon. These materials are usually polycrystalline or amorphous thin films. Typically thin-film stresses exist in these materials, which arise from thermal expansion mismatches and unfavourable energetic configuration after deposition [5]. Micromachinists often try to minimize these stresses, and a slight tensile stress is usually preferred to compressive stress. Two notable thin films which are used as structural layers in surface micromachining are micromechanical or fine-grained polysilicon and low-stress nitride.

Micromechanical or fine-grained polysilicon [7, 8], is formed by low-pressure chemical-vapour deposition (LPCVD) from decomposition of silane (SiH_4) gas at below 600°C . As deposited, the films are amorphous and compressive, but after a 1050°C anneal in N_2 for 3 h the films become polycrystalline and nearly stress-free. While

polysilicon has gauge factors that are significantly less than those of single-crystal silicon [9, 10], the TCR can be made positive, negative, or nearly zero by tailoring processing [9, 11].

LPCVD silicon nitride (Si_3N_4) is an amorphous material which is deposited by reacting dichlorosilane (SiH_2Cl_2) and ammonia (NH_3) gases. Stoichiometric silicon nitride, Si_3N_4 , has high tensile stress of 1–2 GPa as deposited. Silicon rich nitrides, or low-stress nitrides, are deposited by adjusting the gas ratio of $\text{SiH}_2\text{Cl}_2 : \text{NH}_3$ from 1:3–1:4 to 4:1 and depositing at 835 °C. They have much lower stresses, of the order of 10–100 MPa [12].

2.2. Piezoresistive sensors

Following the invention of the bipolar transistor in 1947, a great deal of effort was put into characterizing the properties of single-crystal semiconductors [13]. In 1954, Smith reported the piezoresistive effect of silicon and germanium, which is a change of resistance with applied stress. This discovery enabled production of semiconductor-based sensors [14]. Piezoresistive pressure sensors have piezoresistors mounted on or in a diaphragm. For thin diaphragms and small deflections, the resistance change is linear with applied pressure.

Silicon strain-gauge, metal-diaphragm sensors were first introduced commercially in 1958 [15]. In these early sensors high-cost, low-volume biomedical [16, 17] and aerospace [17] applications were targeted. This trend continued into the 1970s [18–22] when microsensor companies began to move toward higher-volume, lower-cost applications [23], specifically, the automotive industry [22]. Into the 1980s and the present, biomedical and automotive applications are some of the most widely reported in the literature.

The evolution of piezoresistive pressure sensor technology is illustrated in figure 3, starting with metal-diaphragm sensors with bonded silicon strain gauges (figure 3(a)). The strain gauges were bonded by epoxies, phenolics, or eutectics [17]. These first designs had low yield and poor stability due to such factors as thermal mismatch with the metal–epoxy–silicon interface [15].

Metal diaphragms were quickly superseded by single-crystal diaphragms with diffused piezoresistors (figure 3(b)). These new types of sensor had many advantages related to the properties of silicon and the availability of high-quality silicon substrates. Hysteresis and creep associated with metal diaphragms were eliminated. At low temperatures (<500 °C), silicon is perfectly elastic and will not plastically deform [18], but instead will fracture in a brittle manner. Silicon obeys Hooke's law up to 1% strain, a tenfold increase over common metal alloys [18]. Also, the ultimate tensile strength of silicon can be three times higher than that of stainless steel wire [6]. As a piezoresistive material, silicon has gauge factors that are over an order of magnitude higher than those of metal alloys [14].

Some of the first silicon diaphragms were created by mechanical milling spark machining followed by wet chemical isotropic etching, to create a cup shape (figure 3(b)) [16]. These diaphragms were bonded to silicon

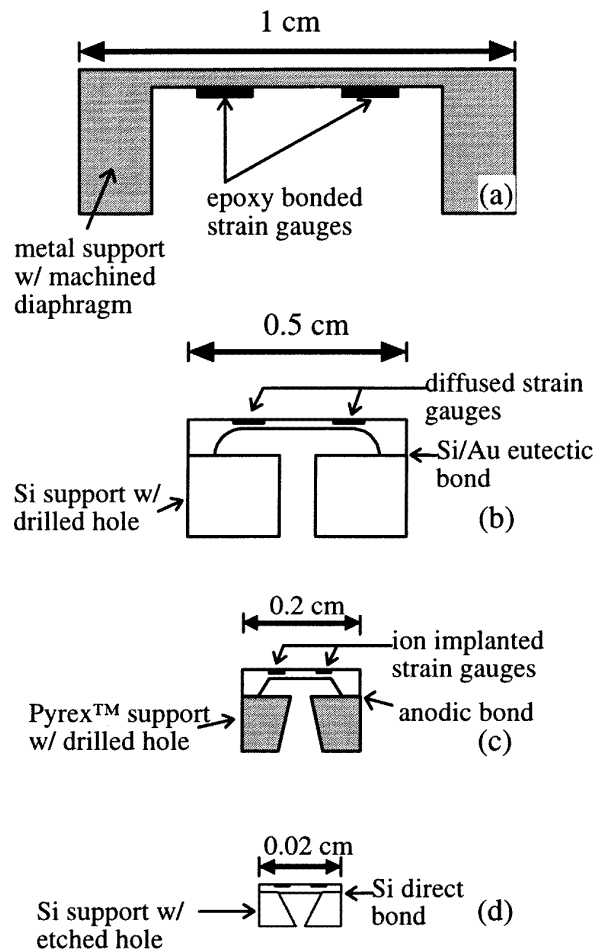


Figure 3. The evolution of diaphragm pressure sensors (adapted from [15]).

supports by a gold–silicon eutectic ($T_{eutectic} = 370^\circ\text{C}$). While this technique of fabrication had the advantages of increased sensitivity and reduced size, cost was still high, and diaphragms were created one at a time, rather than in batch mode.

By the late 1960s and early 1970s, three key technologies were being developed: anisotropic chemical etching of silicon [24–26], ion implantation, and anodic bonding [27, 28]. Ion implantation was used to place strain gauges in single-crystal silicon diaphragms. Ion implantation is generally better than diffusion for doping because both the doping concentration and doping uniformity are more tightly controlled [29]. Anisotropic etching improved the diaphragm fabrication process in a number of ways:

- (i) diaphragm sizes and locations were now well controlled by IC photolithography techniques;
- (ii) strain gauge placements were improved;
- (iii) anisotropic etching was well suited to batch fabrication, allowing hundreds of diaphragms to be created simultaneously; and
- (iv) overall size was decreased further.

Anodic bonding, which uses voltages (500–1500 V) and heat (400–600 °C), was used to bond finished silicon

diaphragm wafers to Pyrex glass supports. Several types of glass formulations designed to reduce thermal mismatch to silicon were used. Anisotropic etching and anodic bonding are batch techniques, and hence hundreds (or more) of pressure sensors could be manufactured simultaneously on a single wafer. This amounted to a significant cost reduction. A representative sensor from this period is shown in figure 3(c).

The 1980s to the present has been called the micromachining period [15], since diaphragm dimensions are shrinking to hundreds of micrometres and minimum feature sizes are shrinking to micrometres (figure 3(d)). Also, anisotropic etching [30–33] and bonding technologies are being improved. In 1985, the direct bonding method was first reported [34]. This method was first used for making silicon-on-insulator (SOI) material, but was quickly applied to micromachined devices [35]. Also, surface-micromachined devices have been reported, which have silicon nitride [36–38] or polysilicon [11, 39, 40] diaphragms. These sensors decrease required die size and may simplify integration with electronics, but at the cost of reduced sensitivity and reproducibility of mechanical properties.

2.3. Capacitive sensors

Capacitive sensors are based upon parallel plate capacitors. A typical bulk-micromachined capacitive pressure sensor is shown in figure 4. The capacitance, C , of a parallel plate capacitor is given by

$$C = \frac{\varepsilon A}{d} \quad (3)$$

where ε , A , and d are the permittivity of the gap, the area of the plates, and the separation of the plates, respectively. For a circular diaphragm sensor under deflection, the capacitance becomes

$$C = \iint \frac{\varepsilon}{d - w(r)} r \, dr \, d\theta \quad (4)$$

where $w(r)$ is the deflection of the diaphragm given by equation (1). Equation (4) is plotted in figure 5 along with a linear least-squares fit. The largest deviation of the fit is 1.5%, which is quite small when compared to the error in the small deflection model of 11% at $w = \frac{1}{2}h$ [4].

A capacitive sensor can be operated in contact mode to increase linearity (figure 6). In contact mode, the capacitance is nearly proportional to the contact area, which in turn exhibits good linearity with respect to applied pressure [41]. This holds true over a wide range of pressures. However, this linearity comes at the expense of decreased sensitivity.

Another method for achieving a linear response is to use bossed diaphragms. Figure 7 illustrates this concept. On the left is a cut-away view of a uniform-thickness diaphragm and its corresponding cross-sectional deflected mode shape. A non-uniform, bossed diaphragm is on the right. The thicker centre portion (or boss) is much stiffer than the thinner tether portion on the outside. The centre boss contributes most of the capacitance of the structure

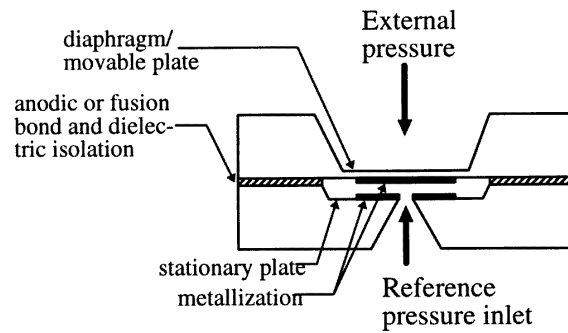


Figure 4. A cross section schematic diagram of a bulk-micromachined, capacitive pressure sensor (adapted from [22]).

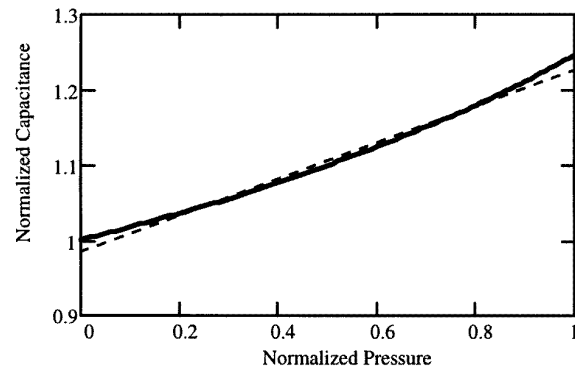


Figure 5. A capacitance–pressure curve for a circular diaphragm with zero built-in stress.

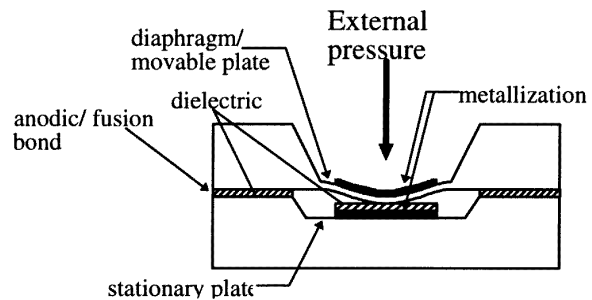


Figure 6. A cross section schematic diagram of a bulk-micromachined, contact-mode pressure sensor.

and its shape does not distort appreciably under applied load. Hence the capacitance–pressure characteristics will be more linear [42–45].

The principal advantages of capacitive pressure sensors over piezoresistive pressure sensors are increased pressure sensitivity and decreased temperature sensitivity [22, 46–49]. However, excessive signal loss from parasitic capacitance is a serious disadvantage, which hindered the development of miniaturized capacitive sensors until on-chip circuitry could be fabricated [46].

Historically, capacitive sensors have benefited from the same advances in diaphragm etching and wafer bonding that piezoresistive sensors have. However, the piezoresistive approach generally has a complex transducer with simple

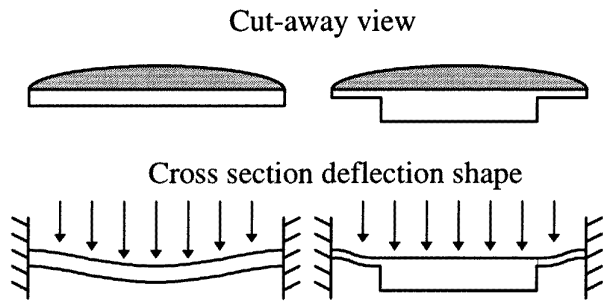


Figure 7. A comparison of deflection shapes for uniform-thickness (left) and bossed (right) diaphragms.

circuit requirements, while the converse is true of the capacitive approach. For this reason, capacitive sensors have benefited more from advances in circuit design than piezoresistive sensors [48].

2.4. Optical

Many diaphragm-based optical sensors have been reported which measure pressure induced deflections by Mach-Zehnder interferometry [50–52] and Fabry-Pérot interferometry [53]. The deflection derived from these devices varies linearly with pressure as witnessed by equation (1). Sensors which measure quantum-well spectrum deformation have also been demonstrated [54].

Optical sensors can be quite accurate, but often suffer from temperature sensitivity problems [55]. Furthermore, aligning the optics and calibrating the sensors can be challenging and expensive.

2.5. Resonance

A new class of pressure sensor has been reported in recent years: the resonant beam pressure sensor. These sensors operate by monitoring the resonant frequency of an embedded doubly clamped bridge [56–58] or comb drive [59], as shown schematically in figure 8. The resonant beam, which has also been called a resonating beam force transducer [60], acts as a sensitive strain gauge [61]. As the stress state of the diaphragm changes, the tension in the embedded structures changes and so does the resonant frequency.

There have been several mechanisms reported by which the structures can be driven into resonance while the resonant frequency is sensed. One method is electrostatic excitation and piezoresistive sensing: the structure is driven to resonance by AC applied voltages, and the resonant frequency is measured by piezoresistors [56, 57]. Structures can also be optically excited by laser and sensed by a photodetector [58], or electrostatically excited and capacitively sensed [59]. Resonant pressure sensors have been shown to exhibit better pressure sensitivity and lower temperature sensitivity than pure piezoresistive sensors. Furthermore, a frequency output is more immune to noise than classical analogue piezoresistive and capacitive signals [56].

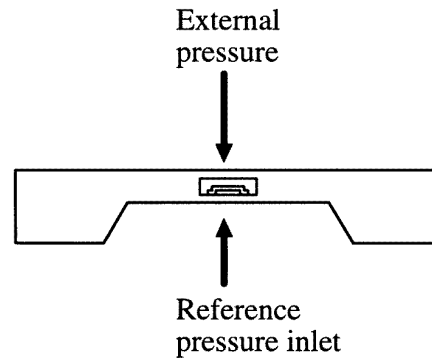


Figure 8. A cross section schematic diagram of a resonant beam pressure sensor (not to scale).

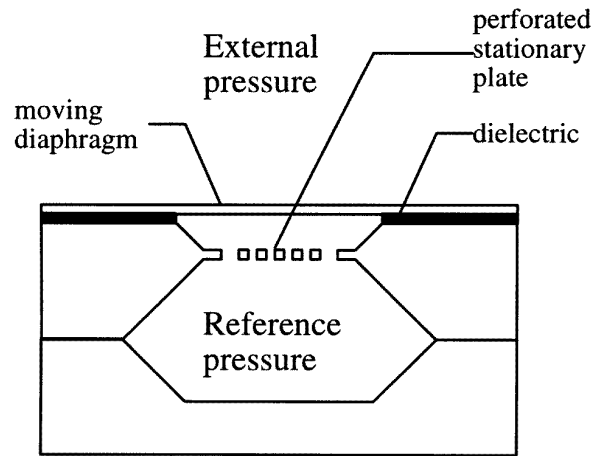


Figure 9. A condenser microphone with a perforated backplate (similar to [65]).

2.6. Microphones and hydrophones

Most microphones reported in the literature are condenser (capacitive) microphones [62]. They operate similarly to capacitive pressure sensors previously described. However, the frequency response and mechanical sensitivity of common capacitive static pressure sensors are inadequate for use as microphones [63]. This is due to acoustic resistance and squeeze-film damping between the movable and stationary plates of the sensor. These effects are reduced by perforating the stationary plate, so that air can escape into a larger chamber [62–64]. Such a device, implemented in bulk micromachining, is shown in figure 9. With proper design, condenser microphones can have the advantages of high stability and flat frequency response [63].

While condenser microphones are more common, piezoresistive [65, 66], and piezoelectric microphones [67–69] have been reported.

At least one micromachined hydrophone has been reported [70, 71]. This hydrophone was based on a condenser microphone and filled with a variety of compressible fluids. The frequency response was as high as 2 kHz.

3. Recent developments

Over the past several years, surface-micromachined pressure sensors have been fabricated and tested at the Microelectronics Development Laboratory within Sandia National Laboratories. These sensors have been based on both silicon nitride and polysilicon diaphragms, and in planar and non-planar versions. Fabrication details and sensor characteristics have been reported elsewhere for non-planar [72,73] and planar [74,75] sensors. The principal advantage of planar sensors is improved manufacturability by reduction of topography, which leads to improvements in photolithography, dry-etch, ion implantation, and metallization processes. Furthermore increased mechanical robustness of similar devices has been demonstrated [76].

Figure 10 contrasts the two types of sensor. The sensors have the same basic piezoresistor and metallization layout, but differ in structure. Both sensors have evacuated reference pressure cavities underneath them. In the non-planar version (top), the cavity is formed above the surface of the wafer by a $2\ \mu\text{m}$ thick sacrificial oxide. This sacrificial oxide, combined with the thickness of the sensor diaphragm itself, is responsible for much of the topography. In the planar sensor, the sacrificial oxide has been embedded in a sub-surface trench which has been planarized by chemical mechanical polishing [75].

Output characteristics of planar pressure sensors are shown in figure 11 for nitride (top) and polysilicon (bottom) diaphragms. Four sizes of pressure sensors are shown in each graph: 50, 100, 150, and 200 μm diameters. The nitride diaphragm sensors exhibit sensitivity clustering at low pressure for the 100, 150, and 200 μm diameter diaphragms: that is the slopes of the output curves for all of these sizes are similar. This behaviour is due to built-in stress effects and large deflections [77] not accounted for by thin-plate theory. The rollover in the 150 and 200 μm diameter sensors is due to the diaphragm contacting the substrate.

Polysilicon-diaphragm-based sensors display more linear and differentiated characteristics than the nitride sensors. The cause is twofold: first the polysilicon diaphragms are $2.3\ \mu\text{m}$ thick, compared to a $1.4\ \mu\text{m}$ thickness of the nitride diaphragms. This causes them to be stiffer and less likely to go into the large-deflection regime. Second, micromechanical polysilicon has far less stress, $<1\ \text{MPa}$, than low-stress nitride (10–100 MPa), which prevents sensitivity clustering. The negative output of the 200 μm diameter polysilicon sensor is due to an incomplete sacrificial oxide etch, which left an oxide island in underneath the centre of the diaphragm, thereby rendering the circumferential resistors inactive.

Work is ongoing towards monolithically integrating these sensors with controlling CMOS electronics. Also, capacitive devices are under development. One of the advantages of capacitive devices is the monotonic increase with applied pressure, even if the diaphragm deflects to contact the substrate [41]. In contrast the piezoresistive devices of figure 11 have a non-monotonic response.

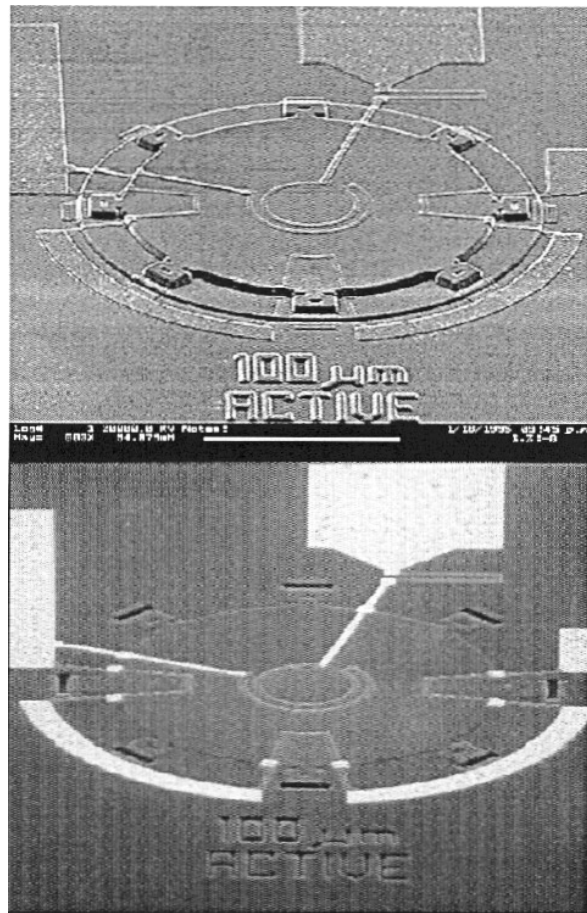


Figure 10. Finished non-planar (top) and planar (bottom) 100 μm diameter pressure sensor diaphragms.

4. Advantages of micromachined sensors

In general for a new product to gain market acceptance, it must pass the 20% rule of thumb: it must be either 20% less expensive or perform 20% better for the same price than an existing product. Many MEMS devices will meet or exceed both requirements simultaneously [78]. As noted before, the 1995 market for micromachined pressure sensors was approximately \$US 1 billion, and is expected to grow to \$US 2.5 billion by 2005 [1]. Furthermore, the total MEMS industry as a whole is expected to grow from \$US 1.5 billion in 1995 to approximately \$US 10 billion by 2000 [79]. While actual future market size is debatable, most agree that the market will grow at a large rate [78]. A few potential advantages of micromachined sensors over their macro-scale counterparts are discussed in this section: leveraging from the IC industry, small form factor, and monolithic integration.

4.1. Leveraging from the IC industry

Most of the advantages of micromachined pressure sensors stem from the fact that many of the manufacturing processes and tools are borrowed from the integrated circuit (IC) industry, such as photolithography, oxidation and diffusion, wet cleaning and etching, thin-film deposition,

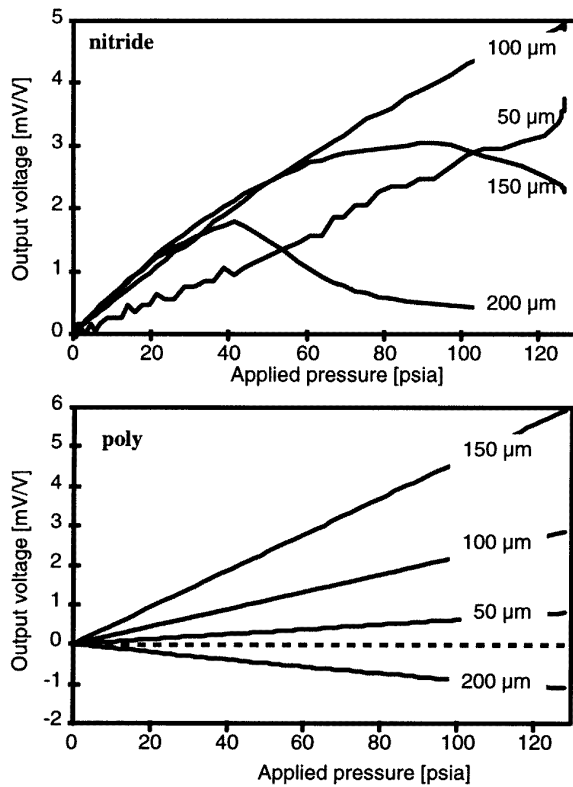


Figure 11. Output characteristics for silicon-nitride- (top) and polysilicon- (bottom) based planar pressure sensors.

metallization, ion implantation, and others. Many of these are used directly, while others have been modified or developed to meet the specific needs of micromachined devices [80]. This leveraging from a large industrial base reduces development costs. In addition, IC fabrication consists of batch processes: hundreds to thousands of units are simultaneously created on a single wafer; wafers are typically processed in lots of 25–100 [1]. The net result is large volume and low unit cost. For example low-cost, disposable, catheter blood pressure sensors are now available in volume [1,81], as are tyre pressure gauges which cost about \$US 10 [82].

High volumes are not only enabled by IC batch techniques, they are also required in order to achieve low cost. Despite the leveraging effect, overhead costs are still high. It is well known that in the IC industry the price of admission—equipment, clean-room facilities, and highly trained staff—is prohibitive, with the newest IC foundries costing in excess of billions of \$US to build and equip. Fortunately the actual cost of a micromachining facility is actually orders of magnitude less, since micromachinists typically use existing foundries or equipment sets that are at least one or two generations behind the state of the art. Nevertheless, the high overhead costs of using microfabrication techniques makes the cost of doing business roughly independent of the number of devices produced [5]. Hence high throughput without sacrificing quality is a major goal of manufacturers.

Complicating the high-volume–low-cost equation that holds true for ICs are the requirements of packaging and

testing of micromachined sensors. While the packaging and testing of ICs is currently highly automated, packaging, functional testing, and calibration of sensors require exposure to the measurand—in this case pressure. Existing IC test equipment is poorly suited to modification for pressure inputs. Trimming and calibration is commonly performed for every part. All told, packaging and testing can account for 75% of the manufacturing cost of a micromachined sensor [83]. Because of these complications, it is generally agreed that designing the package should be carried out at the same time as designing the transducer itself [84].

4.2. Small form factor

For some applications size and weight constraints may be as important as or more important than cost. For these applications, micromachined devices enable not only multiple sensors where there was once only one, but also entirely new sensing functions. In aeronautical, automotive, and space applications, there exists the simultaneous desire for decreased weight and increased instrumentation to achieve the goals of better control and efficiency. The current ‘faster, farther, cheaper’ philosophy of NASA requires drastic reduction of launch weights, which in turn requires reduction of instrumentation weight or quantity or both [85]. In biomedicine, catheter-based devices must occupy small volume, or they cannot be used at all.

4.3. Monolithic integration

The final potential advantage, the prospect of integrating electronics and microsensors on the same substrate, is commercially viable for some products but not for others. For piezoresistive pressure sensors, control circuits are not essential. However, for capacitive pressure sensors, signal-degrading parasitic capacitances are significant and on-chip signal conditioning is desirable. Commercially available micromachined accelerometers used for airbag deployment in automobiles provide a good example. Of several companies producing capacitive micromachined accelerometers, Analog Devices has a one-chip solution [86], whereas Ford Microelectronics [87] and Motorola [88] both use dual-chip, single-package solutions, with the electronics on one chip and the micromechanics on the other.

5. Outlook

Results from surface-micromachined pressure sensors at Sandia National Laboratories illustrate some of the promise and pitfalls of MEMS technologies. While IC technologies are used to advantage in MEMS processing, the thermal and mechanical properties of MEMS materials must be understood, measured, and optimized to achieve accuracy and reproducibility.

Micromachined pressure sensors have an established portion of a large market which will grow for the foreseeable future. Monolithic integration of piezoresistive, capacitive, optical, and resonant pressure sensors with controlling electronics and/or optics will become increasingly common.

Acknowledgments

The authors are indebted to the process development engineers, operators, and technicians of Sandia's Microelectronics Development Laboratory for their contributions to the process development and fabrication of the surface-micromachined pressure sensors. This work was supported by the United States Department of Energy under contract DE-AC04-94AL85000. Sandia is a multiprogramme laboratory operated by Sandia Corporation, a Lockheed Martin Company, for the United States Department of Energy.

References

- [1] Bryzek J 1996 MEMS: a closer look at part 2: the MEMS industry in Silicon Valley and its impact on sensor technology *Sensors* July 4
- [2] Oliver F J 1971 *Practical Instrumentation Transducers*
- [3] Mastrangelo C H 1991 Thermal applications of microbridges *PhD Thesis* University of California at Berkeley
- [4] Timoshenko S and Woinosky-Krieger S 1987 *Theory of Plates and Shells*
- [5] Mastrangelo C H and Tang W C 1994 Semiconductor sensor technologies *Semiconductor Sensors* ed S M Sze pp 17–84
- [6] Petersen K E 1982 Silicon as a mechanical material *Proc. IEEE* **70** 420–57
- [7] Guckel H, Burns D W, Rutigliano C R, Showers K and Uglow J 1987 Fine-grained polysilicon and its application to planar pressure transducers *Tech. Digest 4th Int. Conf. on Solid-State Sensors and Actuators Transducers '87* pp 277–82
- [8] Guckel H, Sniogowski J J and Christenson T R 1989 Fabrication of micromechanical devices from polysilicon films with smooth surfaces *Sensors Actuators* **20** 117–22
- [9] French P J and Evans A G R 1989 Piezoresistance in polysilicon and its applications to strain gauges *Solid-State Electron.* **32** 1–10
- [10] Gridchin V A, Lubimsky V M and Sarina M 1995 Piezoresistive properties of polysilicon films *Sensors Actuators A* **49** 67–72
- [11] Burns D W 1988 Micromechanics of integrated sensors and the planar processed pressure transducer *PhD Thesis* University of Wisconsin—Madison
- [12] Sekimoto M, Yoshihara H and Ohkubo T 1982 Silicon nitride single-layer x-ray mask *J. Vac. Sci. Technol.* **21** 4
- [13] Sze S M 1994 Classification and terminology of sensors *Semiconductor Sensors* ed S M Sze pp 1–15
- [14] Smith C S 1954 Piezoresistance effect in germanium and silicon *Phys. Rev.* **94** 42–9
- [15] Bryzek J, Petersen K, Mallon J R, Christel L and Pourahmadi F 1990 *Silicon Sensors and Microstructures*
- [16] Peake E R, Zias A R and Egan J V 1969 Solid-state digital pressure transducer *IEEE Trans. Electron Devices* **ED-16** 870–6
- [17] Sanchez J C 1963 Semiconductor strain-gage pressure sensors *Instruments and Control Systems*. pp 117–20
- [18] Gieles A C M and Somers G H J 1973 Miniature pressure transducers with a silicon diaphragm *Philips Tech. Rev.* **33** 14–20
- [19] Samaun, Wise K D and Angell J B 1973 An IC piezoresistive pressure sensor for biomedical instrumentation *IEEE Trans. Biomed. Eng.* **BME-20** 101–9
- [20] Borky J M and Wise K D 1979 Integrated signal conditioning for silicon pressure sensors *IEEE Trans. Electron Devices* **ED-26** 1906–10
- [21] Ko W S, Hyneczek J and Boettcher S F 1979 Development of a miniature pressure transducer for biomedical application *IEEE Trans. Electron Devices* **ED-26** 1896–905
- [22] Clark S K and Wise K D 1979 Pressure sensitivity in anisotropically etched thin-diaphragm pressure sensors *IEEE Trans. Electron Devices* **ED-26** 1887–96
- [23] Meindl J D and Wise K D 1979 Foreword *IEEE Trans. Electron Devices* **ED-26** 1861–3
- [24] Kendall D L 1975 On etching very narrow grooves in silicon *Appl. Phys. Lett.* **26** 195–201
- [25] Bean K E 1978 Anisotropic etching of silicon *IEEE Trans. Electron Devices* **ED-25** 1185–93
- [26] Bassous E 1978 Fabrications of novel three-dimensional microstructures by the anisotropic etching of (100) and (110) silicon *IEEE Trans. Electron Devices* **ED-25** 1178–85
- [27] Pomerantz D I 1968 Anodic bonding *US Patent* 3 397 278
- [28] Wallis G and Pomerantz D I 1969 Field assisted glass–metal sealing *J. Appl. Phys.* **40** 3946–9
- [29] Ghandi S K 1983 *VLSI Fabrication Principles*
- [30] Puers B and Sansen W 1990 Compensation structures for convex corner micromachining in silicon *Sensors Actuators A* **21–23** 1036–41
- [31] Offereins H L, Khl K and Sandmaier H 1991 Methods for the fabrication of convex corners in anisotropic etching of (100) silicon in aqueous KOH *Sensors Actuators A* **25–27** 9–13
- [32] Mayer G K, Offereins H L, Sandmaier H and Khl K 1990 Fabrication of non-underetched convex corners in anisotropic etching (100) silicon in aqueous KOH with respect to novel micromechanic elements *J. Electrochem. Soc.* **137** 3947–50
- [33] Bao M, Burren C, Esteve J, Bausells J and Marco S 1993 Etching front control (100) strips for corner compensation *Sensors Actuators A* **37/38** 727–32
- [34] Lasky J B, Stiffler S R, White F R and Abernathy J R 1985 Silicon-on-insulator (SOI) by bonding and etch-back *Tech. Digest 9185 IEEE Int. Electron Device Meeting (IEDM 85)* pp 684–7
- [35] Petersen K E, Barth P W, Poydock J, Brown J, Mallon J and Bryzek J 1988 Silicon fusion bonding for pressure sensors *Tech. Digest 1988 Solid State Sensor and Actuator Workshop (Hilton Head, SC, 1988)* p 144
- [36] Sugiyama S, Suzuki T, Kawahata K, Shimaoka K, Takigawa M and Igarashi I 1986 Micro-diaphragm pressure sensor *Tech. Digest 1986 Int. Electron Devices Meeting (IEDM '86)* pp 184–7
- [37] Sugiyama S, Shimaoka K and Tabata O 1991 Surface micromachined micro-diaphragm pressure sensors *Digest Tech. Papers 1991 Int. Conf. on Solid-State Sensors and Actuators (Transducers '91)* pp 188–91
- [38] Shimaoka K, Tabata O, Kimura M and Sugiyama S 1993 Micro-diaphragm pressure sensor using polysilicon sacrificial layer etch-stop technique *Tech. Digest 7th Int Conf. on Solid-State Sensors and Actuators (Transducers '93)* pp 632–5
- [39] Guckel H and Burns D W 1986 Fabrication techniques for integrated sensor microstructures *Tech. Digest IEEE Int. Electron Devices Meeting (IEDM '86)* pp 122–5
- [40] Guckel H 1991 Surface micromachined pressure transducers *Sensors Actuators A* **28** 133–46
- [41] Cho S T, Najafi K and Wise K D 1990 Secondary sensitivities and stability of ultrasensitive silicon pressure sensors *Tech. Digest 1990 IEEE Solid-State Sensor and Actuator Workshop (Hilton Head, SC, 1990)*
- [42] Schöenberg U, Schnatz F V and Brockherde W 1991 CMOS integrated capacitive pressure transducer with on-chip electronics and digital calibration capability *Digest Tech. Papers 1991 Int. Conf. on Solid-State Sensors and Actuators (Transducers '91)* p 304
- [43] Schnatz F V, Schöenberg U, Brokherde W, Kopystynski,

- Mehlorn T, Obermier E and Benzel H 1992 Smart CMOS capacitive pressure transducer with on chip calibration capability *Sensors Actuators A* **34** 77–83
- [44] Zhang Y and Wise K D 1994 Performance of non-planar silicon diaphragms under large deflections *J. Microelectromech. Syst.* **3** 59–68
- [45] Zhang Y and Wise K D 1995 A high-accuracy multi-element silicon barometric pressure sensor *Digest Tech. Papers 1995 Int. Conf. on Solid-State Sensors and Actuators (Transducers '95)* p 608–11
- [46] Frobenius W D, Sanderson A C and Nathanson H C 1973 A microminiature, solid-state capacitive blood pressure sensor transducer with improved sensitivity *IEEE Trans. Biomed. Eng.* **BME-20** 312–4
- [47] Chau H-L and Wise K D 1987 Scaling limits in batch-fabricated silicon pressure sensors *IEEE Trans. Electron Devices* **ED-34** 850–8
- [48] Lee K W and Wise K D 1982 Simsim: a simulation program for solid-state pressure sensors *IEEE Trans. Electron Devices* **ED-29** 34–41
- [49] Sander C S, Knutt J W and Meindl J D 1980 A monolithic capacitive pressure sensor with pulse-period output *IEEE Trans. Electron Devices* **ED-27** 927–30
- [50] Wagner D, Frankenberger J and Deimel P 1994 Optical pressure sensor using two Mach–Zehnder interferometers for the TE and TM polarizations *J. Microelectromech. Microeng.* **4** 35–9
- [51] Dzuiban J A, Gorecka-Drzazga A and Lipowics U 1992 Silicon optical pressure sensor *Sensors Actuators A* **32** 628–31
- [52] Hoppe K, Anderson L U A and Bouwstra S 1995 Integrated Mach–Zehnder interferometer pressure transducer *8th Int. Conf. on Solid-State Sensors and Actuators (Transducers '95)* pp 590–5
- [53] Chan M A, Collins S D and Smith R L 1994 A micromachined pressure sensor with fiber-optic interferometric readout *Sensors Actuators A* **43** 196–201
- [54] Sosin T, Perlin, Trzeciakowski W and Tober R 1994 New results on optical pressure sensors based on semiconductor quantum well *Sensors Actuators A* **42** 654–7
- [55] Bartelt H and Unzeitig H 1993 Design and investigation of micromechanical bridge structures for an optical pressure sensor with temperature compensation *Sensors Actuators A* **37–38** 167–70
- [56] Petersen K E, Pourahmadi F, Brown J, Parsons, Skinner M and Tudor J 1991 Resonant beam pressure sensor with silicon fusion bonding *Digest Tech. Papers 1991 Int. Conf. on Solid-State Sensors and Actuators (Transducers '91)* pp 664–7
- [57] Burns D W, Zook J D, Horning R D, Herb W R and Guckel H 1994 A digital pressure sensor based on resonant microbeams *Tech. Digest 1994 Solid-State Sensor and Actuator Workshop (Hilton Head, SC, 1994)* pp 221–4
- [58] Burns D W, Zook J D, Horning R D, Herb W R and Guckel H 1995 Sealed-cavity resonant microbeam pressure sensor *Sensors Actuators A* **48** 179–86
- [59] Welham C J, Gardner J W and Greenwood J 1995 A laterally driven micromachined resonant pressure sensor *Digest Tech. Papers 8th Int. Conf. on Solid-State Sensors and Actuators (Transducers '95)* pp 586–9
- [60] Sniogowski J J 1991 Design and fabrication of the polysilicon resonating beam force transducer *PhD Thesis* University of Wisconsin—Madison
- [61] Zook J D, Burns D W, Guckel H, Sniogowski J J, Engelstad R L and Feng Z 1992 Characteristics of polysilicon resonant microbeams *Sensors Actuators A* **35** 51–9
- [62] Scheeper P R, Olthuis W and Bergveld P 1994 Improvement of the performance of microphones with a silicon nitride diaphragm and backplate *Sensors Actuators A* **40** 179–86
- [63] Bergqvist J, Rudolf F, Maisano J, Parodi F and Rossi M 1991 A silicon condenser microphone with a highly perforated backplate *Digest Tech. Papers 1991 Int. Conf. on Solid-State Sensors and Actuators (Transducers '91)* pp 266–9
- [64] Bergqvist J and Gobet J 1994 Capacitive microphone with a surface micromachined backplate using electroplating technology *J. Microelectromech. Syst.* **3** 69–75
- [65] Kälvesten D, Löfdahl L and Stemme G 1995 Small piezoresistive microphones specially designed for the characterization of turbulent gas flow *Sensors Actuators A* **46/47** 151–5
- [66] Schellin R, Strecker M, Nothelfer U and Schuster G 1995 Low pressure acoustic sensors for airborne sound with piezoresistive monocrystalline silicon and electrochemically etched diaphragm *Sensors Actuators A* **46/47** 156–60
- [67] Kim E S, Kim J R and Muller R S 1991 Improved IC-compatible piezoelectric microphone and CMOS process *Digest Tech. Papers 1991 Int. Conf. on Solid-State Sensors and Actuators (Transducers '91)* pp 270–3
- [68] Pied R, Kim E S, Hong D H and Muller R S 1993 Piezoelectric microphone with on-chip CMOS circuits *J. Microelectromech. Syst.* **2** 111–20
- [69] Kim E S, Muller R S and Hjian R S 1992 Front-to-backside alignment using resist-patterned etch control and one etching step *J. Microelectromech. Syst.* **1** 95–9
- [70] Bernstein J 1991 A micromachined condenser hydrophone *Tech. Digest IEEE Solid State Sensor and Actuator Workshop (Hilton Head, SC, 1992)* pp 161–5
- [71] Bernstein J, Weinberg M, McLaughlin E, Powers J and Tito F 1994 Advanced micromachined condenser hydrophone *Tech. Digest 1994 Solid-State Sensor and Actuator Workshop (Hilton Head, SC, 1994)* pp 73–7
- [72] Eaton W P and Smith J H 1995 A CMOS-compatible surface-micromachined pressure sensor for aqueous ultrasonic application *Proc. Smart Structures and Materials 1995 SPIE* vol 2448 (Bellingham, WA: SPIE) pp 258–65
- [73] Eaton W P and Smith J H 1995 Characterization of a surface micromachined pressure sensor array *Proc. 1995 Micromachining and Microfabrication Symp. SPIE* vol 2642 (Bellingham, WA: SPIE) pp 256–64
- [74] Nasby R D, Hetherington D L, Sniogowski J J, Apblett C A, Smith J H, Barron C C, Eaton W P and McWhorter P J 1996 Application of chemical mechanical polishing to planarization of surface-micromachined devices *Tech. Digest 1996 Solid State Sensors and Actuators Workshop (Hilton Head, SC, 1996)* pp 48–53
- [75] Eaton W P and Smith J H 1996 Planar surface-micromachined pressure sensor with a sub-surface reference pressure cavity *Proc. Micromachined Devices and Components II (Austin, TX), SPIE* vol 2882 (Bellingham, WA: SPIE) pp 259–65
- [76] Yang X and Tai Y C 1996 Improved boundary conditions of surface micromachined diaphragms *Micromachining Workshop III Abstracts (1996)*
- [77] Suhir E 1991 *Structural Analysis in Microelectronic and Fiber-Optic Systems* vol 1
- [78] Walsh S 1996 Commercialization MEMS—too fast or too slow? *Micromachined Devices and Components II SPIE* vol 2882, pp 12–24
- [79] Schumann E 1995 Creating the market for MEMS devices *SEMI Market Survey*
- [80] Kloeck B and de Rooij N F 1994 Mechanical sensors *Semiconductor Sensors* ed S M Sze, pp 153–99
- [81] Bryzek J 1996 Impact of MEMS technology on society *Sensors Actuators A* **56** 1–10
- [82] Petersen K 1995 MEMS: what lies ahead *Digest Tech. Papers 1995 Int. Conf. on Solid-State Sensors and*

- Actuators (Transducers '95)* pp 894–7
- [83] de Lambilly H, Grace R and Sidhu K 1996 Package or perish *Proc. 1996 Sensors Expocon* p 275
- [84] Senturia S D and Smith R L 1988 Microsensor packaging and partitioning *Sensors Actuators* **15** 221–34
- [85] Grunthaler F 1996 Plenary talk *Proc. Micromachining Workshop III (Anaheim, CA, 1996)*
- [86] 1995 ADX105 $\pm 1g$ to $\pm 5g$ single chip accelerometer with signal conditioning *I Analog Devices Specification Sheet*
- [87] Spangler L and Kemp C J 1996 A smart automotive accelerometer with on-chip airbag development circuits *Tech. Digest 1996 Solid-State Sensor and Actuator Workshop (Hilton Head, SC, 1996)* pp 211–4
- [88] Preliminary information, XMMAS series micromachined accelerometers *I Motorola Specification Sheet*